Relax

User Manual
Version 1

www.geodynamics.org

Sylvain Barbot

Relax: Nonlinear Postseismic Relaxation in the Fourier Domain

User Manual

Sylvain Barbot (sbarbot@caltech.edu)

Division of Geological and Planetary Sciences, Caltech

Oct. 11th, 2011, last revision Dec. 28th, 2011

1   Introduction

The open-source program RELAX evaluates the displacement and stress in a half space with gravity due to dislocations [e.g., *Okada*, 1992], Mogi sources [*Mogi*, 1958], and surface tractions; and the nonlinear time-dependent deformation that follows due to power-law rheology materials in the bulk and/or rate-strengthening friction faults. The numerical method is based on a Fourier-domain elastic Green's function [*Barbot et al.*, 2009b; *Barbot and Fialko*, 2010a] and an equivalent body-force representation of co-seismic and post-seismic deformation processes [*Barbot et al.*, 2009a; *Barbot and Fialko*, 2010b]. Application of the method for the 2004 Mw 6 Parkfield earthquake can be found in the work of *Barbot et al.* [2009a] and *Bruhat et al.* [2011].

The possible applications for the earthquake-cycle modeling include i) co-seismic displacement and Coulomb stress calculation, ii) quasi-static stress transfer between earthquakes due to a postseismic transient, iii) modeling of postseismic transients including nonlinear rheologies and multiple mechanisms, iv) cycle of multiple earthquakes and spin-up models, v) loading cycle of lakes or the monsoon.

2   Acknowledgment

The cover image is a Paraview visualization of the displacement field produced by the 1992 Mw 7.3 Landers earthquake from the coseismic slip model of *Fialko* [2004]. The coseismic shear stress on the Hector Mine faults is shown on the far right. The streamlines and the vectors indicate the direction of motion. The shadowed neighboring faults are from UCERF 2 and the prisms indicate continuous GPS stations. The model and the visualization can be reproduced using the material provided in the examples.

Contents

3   Theoretical background

3.1   Green's function

The approach used in RELAX to evaluate the three-dimensional displacement in a half space is to solve for the displacement field, for static deformation, or the velocity field, for quasi-static problems, using the elastic Green's function. Static deformation caused by earthquakes and time-dependent processes such as viscoelastic flow, poroelastic rebound and fault afterslip can be represented by equivalent body forces and surface tractions so the methods consists, without loss of generality, in finding the displacement and stress caused by an arbitrary distribution of body forces f_i and surface tractions subjected to a mixed boundary condition with buoyancy. Consider the inhomogeneous Navier's equation

$$\mu \left(\frac{\alpha}{1 - \alpha} u_{j,ij} + u_{i,jj} \right) + f_i = 0 \tag{1}$$

where μ is the shear modulus, α is a dimensionless parameter that can be expressed in terms of the Lamé's parameters or the Poisson's ratio

$$\alpha = \frac{\lambda + \mu}{\lambda + 2\mu} = \frac{1}{2(1 - \nu)} \, , \tag{2}$$

u_i is the displacement (or velocity) and f_i, the internal body force (or force per unit time), subjected to the surface boundary condition

$$q_i + \sigma_{ij} n_j + \Delta \rho \, g \, u_3 n_i = 0, \qquad x_3 = 0 \tag{3}$$

with σ_{ij} the Cauchy stress tensor, $n_i = (0, 0, -1)$ the surface normal vector and $q_i(x_1, x_2)$, the prescribed surface traction. The solution displacement that satisfies eq. (1) and (3) can be decomposed into a homogeneous and a particular contribution

$$u_i = u_i^h + u_i^p \tag{4}$$

where the displacement field u_i^h is a solution of the homogeneous Navier's equation

$$\alpha \, u_{j,ij}^h + (1 - \alpha) \, u_{i,jj}^h = 0 \tag{5}$$

with inhomogeneous surface boundary conditions and the particular solution u^p satisfies eq. (1) regardless of the surface boundary condition. The particular solution can be obtained in the Fourier domain

$$\hat{u}_i^p(k_1, k_2, k_3) = \begin{cases} 0 \, , & k_1 = k_2 = k_3 = 0 \\ \dfrac{1}{\mu} \dfrac{(1 - \alpha) \, k_l k_l \, \delta_{ij} - \alpha \, k_i k_j}{4\pi^2 (k_l k_l)^2} \, \hat{f}_j \, , & \text{otherwise} \end{cases} \tag{6}$$

where the k_i are the wavenumbers and the hats correspond to the Fourier transform of the corresponding variables. The zero wavenumber component of the Fourier solution corresponds to a rigid-body displacement and does not correspond to an elastic deformation. The temporary solution requires the following correction to satisfy the traction boundary condition.

$$
\begin{aligned}
\hat{u}_1^h(k_1, k_2, x_3) &= \big[-2B_1\beta^2 + \alpha\,\omega_1\,(B_1\,\omega_1 + B_2\,\omega_2)(1 + \beta\,x_3) \\
&\qquad + \; \alpha\,i\omega_1\beta\,B_3(1 - \alpha^{-1} + \beta x_3) \big]\,e^{-\beta\,x_3} \\
\hat{u}_2^h(k_1, k_2, x_3) &= \big[-2B_2\beta^2 + \alpha\,\omega_2\,(B_1\,\omega_1 + B_2\,\omega_2)(1 + \beta\,x_3) \\
&\qquad + \; \alpha\,i\omega_2\beta\,B_3(1 - \alpha^{-1} + \beta x_3) \big]\,e^{-\beta\,x_3} \\
\hat{u}_3^h(k_1, k_2, x_3) &= \alpha\,\beta^2 \big[\, i\,(\omega_1 B_1 + \omega_2 B_2)\,x_3 \\
&\qquad - \; B_3\,(\alpha^{-1} + \beta\,x_3)\,\big]\,e^{-\beta\,x_3}
\end{aligned}
\tag{7}
$$

where we have used $\beta = 2\pi \left(k_1^2 + k_2^2 \right)^{1/2}$. The values of the B_i are chosen to satisfy the inhomogeneous boundary condition

$$B_1(k_1, k_2) = \frac{\hat{p}_1(k_1, k_2)}{2\mu \, \beta^3}$$

$$B_2(k_1, k_2) = \frac{\hat{p}_2(k_1, k_2)}{2\mu \, \beta^3} \tag{8}$$

$$B_3(k_1, k_2) = \frac{\beta \, \hat{p}_3(k_1, k_2) - i(1 - \alpha)[\omega_1 \hat{p}_1(k_1, k_2) + \omega_2 \hat{p}_2(k_1, k_2)]}{2\mu \, \alpha \, \beta^3 (\beta + \gamma)}$$

where the effective traction $\hat{p}_i$ incorporates external traction and buoyancy

$$\hat{p}_i(k_1, k_2, x_3 = 0) = \hat{t}_i^p + \Delta\rho \, g \, \hat{u}_3^p \, n_i + \hat{q}_i \tag{9}$$

with

$$\hat{u}_3^p(k_1, k_2, x_3 = 0) = \int_{-\infty}^{\infty} \hat{u}_3^p(k_1, k_2, k_3) \, dk_3 \tag{10}$$

and

$$\hat{t}_i^p(k_1, k_2) = \mu \int_{-\infty}^{\infty} \left(k_j \hat{u}_i^p + k_i \hat{u}_j^p - \frac{1 - 2\alpha}{1 - \alpha} k_l \hat{u}_l^p \delta_{ij} \right) n_j \, dk_3 \tag{11}$$

The formulation (7-11) is a solution for the elastic deformation in a homogeneous half space with mixed boundary condition. The solution is evaluated analytically in the Fourier domain and a space-domain solution is obtained with a fast Fourier transform. The advantage is that the performance of the computation scales as $N \log N$, where N is the number of samples in the grid, independently of the number of dislocation. The discrete Fourier transform also introduces periodicity in the solution. In many cases, this is not a desired feature, so the boundaries of the computational domain should be as far as possible from the domain of interest.

3.2 Time integration

The time stepping in RELAX is done by linearizing the time advance using the Runge-Kutta numerical integration scheme with an adaptive time steps. For viscoelastic flow and afterslip, the instantaneous strain rate is a function of stress only so that one can write

$$\dot{\epsilon} = f(t, \epsilon) \tag{12}$$

The second-order Runge-Kutta numerical integration to integrate the $y' = f(t, y)$ can be summarized as follows:

$$\begin{aligned} y_{n+1} &= y_n + k_2 \\ k_1 &= h * f(t_n, y_n) \\ k_2 &= h * f(t_n + h, y_n + k_1) \end{aligned} \tag{13}$$

The scheme is second-order accurate, so reducing the time steps help avoiding numerical instabilities.

3.3 Equivalent body-force representation of dislocation

The slip on a finite fault can be represented by a linear combination of force moments and surface tractions [*Aki and Richards*, 1980]. The method is quite popular in seismology to represent an earthquake as a double-couple point source, but the same representation holds for finite sources. It is possible to express analytically the spatial distribution of body forces and surface traction for a patch of rectangular fault slip. For a vertical rectangular
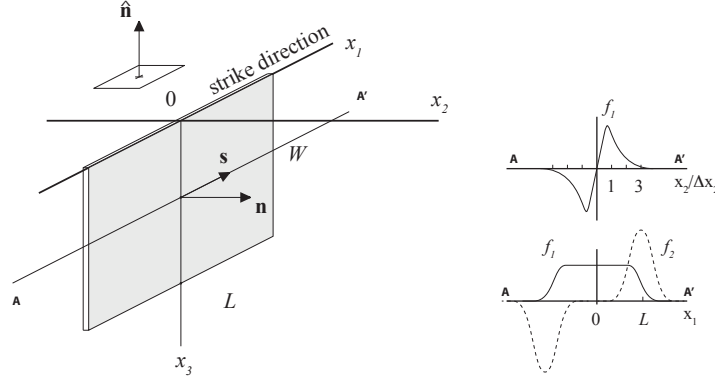
Figure 1: Equivalent body force for a vertical strike-slip fault of length L and width W. The fault slip is tapered with the Ω function of Eq. (15).

strike-slip fault of length L and width W (Figure 1), the body force representation is

$$
\begin{aligned}
f_1(x_1, x_2, x_3) &= -G\,\Omega_\beta\left(\frac{x_1}{L}\right)\frac{\partial}{\partial x_2}\delta_T(x_2)\,\Omega_\beta\left(\frac{x_3}{W}\right)\\[4pt]
f_2(x_1, x_2, x_3) &= -G\,\frac{\partial}{\partial x_1}\Omega_\beta\left(\frac{x_1}{L}\right)\delta_T(x_2)\,\Omega_\beta\left(\frac{x_3}{W}\right)\\[4pt]
f_3(x_1, x_2, x_3) &= 0
\end{aligned}
\tag{14}
$$

where the function $\Omega_\beta(x)$ is the tapered boxcar parameterized with roll-off parameter β

$$
\Omega_\beta(x) =
\begin{cases}
1, & |x| < \dfrac{1-2\beta}{2(1-\beta)}\\[10pt]
\cos\left(\pi\dfrac{(1-\beta)|x| - \frac{1}{2} + \beta}{2\beta}\right)^2, & \\[10pt]
& \dfrac{1-2\beta}{2(1-\beta)} < |x| < \dfrac{1}{2(1-\beta)}\\[10pt]
0, & \text{otherwise}
\end{cases}
\tag{15}
$$

and the function δ is the numerical equivalent to the Dirac's delta function, for example

$$
\delta_T(x) = \frac{1}{T\sqrt{2\pi}}\exp\left(-\frac{x^2}{2T^2}\right)
\tag{16}
$$

In RELAX, the fault thickness is chosen to be the sampling size $T = \Delta x$. A similar relation can be found for faults of arbitrary orientation. The generalization simply involves rotations and translations.

4   Setting up the program

4.1   Introduction

The RELAX code is written in Fortran90 with a few I/O functions written in C. The performance of the code depends greatly on the efficiency of the discrete Fourier transform being used. The program can work with the Cooley-Tukey FFT algorithm, for which the source code is provided. For better performance, it is recommended to use the FFT native to the computer environment. The program can readily use the SGI, the FFTW and the Intel MKL FFTs. While we have found that the Intel MKL FFT provides the most efficient calculation, the package provided by the CIG web site implements FFTW.

Both the post-processing and the storage of the simulation are greatly facilitated by writing output files in the cross-platform NetCDF binary format used by the Generic Mapping Tools (GMT). GMT is convenient to rapidly display the simulation results as it is computed, transform the output into other formats or projections (for example, to project the displacement into the Radar line of sight of a satellite to compare with synthetic aperture radar data), make animations and communicate results. Although RELAX can output in ASCII format, it is recommended to link the code to the GMT 4.5 libraries. A suite of GMT-based post-processing scripts are available in the `util` directory and required GMT to be installed in your system.

The output of the simulation can be projected on the fly to geographic coordinates, which is convenient to communicate results to others in a global coordinate system. In RELAX, this is performed with the proj4 library. It is recommended to install these libraries on your system to facilitate post processing.

4.2   Running

The binary packages provided on the CIG website contain everything needed to run simulations. After unpacking the packages, open a terminal (or, in Windows, a Command Prompt) and run the setup script

```
source setup.sh   # for Linux and Mac on bash
source setup.csh  # for Linux and Mac on csh
setup.bat         # for Windows
```

You should get the response

```
Ready to run Relax.
```

On Linux and Mac, you can check which shell is running (`bash` or `csh`) by typing the command `ps -p $$` in a terminal.

On shared memory machines, such as most modern laptops and desktops, it is possible to run the code in parallel using `openmp`. The number of CPU's used is the maximum number of threads allowed by the machine, or the number found in the environment variable `OMP_NUM_THREADS`. To change the value, type

```
export OMP_NUM_THREADS=4 # for Linux and Mac
set OMP_NUM_THREADS=4    # for Windows
```

on the command line. This command affects all other programs running in this session. On Linux or Mac machines, to set the number for a specific run, prepend the variable definition to your command

```
OMP_NUM_THREADS=4 relax --option
```

Some examples of simple calculations are provided in the `examples` directory. For instance, to run the first example, change into the `examples` directory and run

```
./run1.sh  # for Linux and Mac
./run1.bat # for Windows
```

Alternately, on Windows, you can double-click on `run1.bat` from the file browser.

5   Modeling a deformation scenario

The computation is performed in a uniform Cartesian grid (see Figure 2). The grid is defined by the number of nodes in the three directions (SX1, SX2, SX3). The code is designed to deal with dimensions that are powers of two only: 128, 256 or 512, for example. The spatial extent of the computational domain depends on the sampling intervals, (DX1, DX2, DX3). The horizontal extent of the computational grid is SX1*DX1 and SX2*DX2 , in the x_1 and x_2 directions, respectively. In the depth direction, the computational domain extends from 0 to SX3*DX3/2. The coordinate system is right handed, with x_1 pointing north, x_2 pointing east, and x_3 pointing down.

   All the parameters that control the simulation in the input file are assumed to be in S.I. units. That is, lengths are in meters (m), slip is in meters (m), time is in seconds (m), the elastic moduli are in Pascals (Pa). The user is responsible for making the choice of parameters self consistent. For earthquake cycle simulations, it is common to use km, MPa and year for distance, stress, and time units, respectively.

   To ensure accurate models, the rule of thumb is to have the domain at least ten times the characteristic dimension of the source, or to have any edge of the computational grid about five fault lengths away from a fault tip. Another constraint that ensures good sampling, is to allow for at least five samples per fault. These two constraints can be satisfied simultaneously by maximizing the number of nodes, at the expense of computer memory.
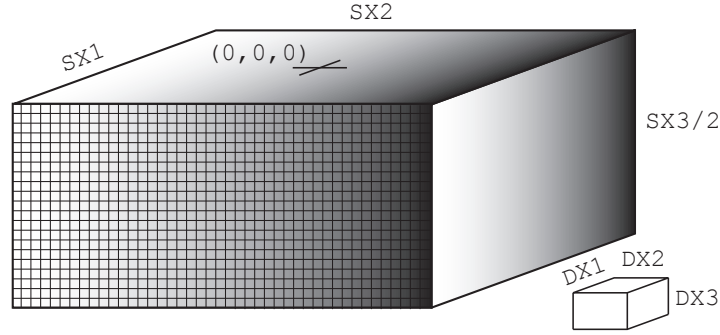

Figure 2: The discretized half space. The origin of the reference system is at the center of the surface. The modeled half space dimension is $-\Delta x_1 \times \mathrm{sx}_1/2$ to $\Delta x_1 \times (\mathrm{sx}_1 - 1)/2$ in the x_1 direction, $-\Delta x_2 \times \mathrm{sx}_2/2$ to $\Delta x_2 \times (\mathrm{sx}_3 - 1)/2$ in the x_2 direction and 0 to $\Delta x_3 \times (\mathrm{sx}_3 - 1)/2$ in the x_3 (depth) direction.

5.1   Fault geometry

Many simulations imply the relaxation of the stress perturbation from a coseismic rupture. A rupture model consists in a collection of slip patches that discretize the fault geometry and the slip distribution. Every slip patch is described by a geologic representation, as shown in Figure 3. A fault segment is modeled by its length in the along-strike direction, its width in the down-dip direction, the position of the top tip (x_s, y_s, and z_s) and its strike and dip angles. By convention, an observer located at the top fault tip and oriented in the strike direction would face the fault trace and would have the fault dipping to his right for a dip angle between $0°$ and $90°$. This is the same convention used by *Okada* [1992], *Wang et al.* [2003] and *Wang et al.* [2006]. In RELAX, to avoid high frequency oscillations near a stress concentration (the so-called Gibbs phenomenon), the slip distribution is smoothed near the fault tip. The amplitude of smoothing is controlled by a roll-off parameter going from $\beta = 0$ for no smoothing to $\beta = 0.5$ for strong smoothing. A value of $\beta = 0.2$ ensures stability of the computation. The seismic moment is conserved for all smoothing values. There is a default value of the smoothing parameter defined at the beginning of the input file

```
# dx1,dx2,dx3,beta (0-0.5),nq
0.5 0.5 0.5 0.2 2
```
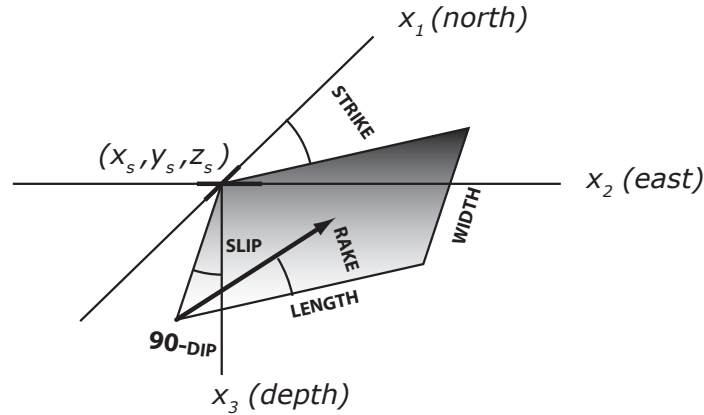
Figure 3: Geologic model of slip on a fault. The fault is described by the position of its top tip, its length in the along-strike direction, width in the down-dip direction, its strike angle and its dip angle. The rake indicates the orientation of slip. For volumes (such as those used to define slabs and shear zones), an extra thickness parameter indicates how the rectangular volume is extruded from its center.

but it can be amended for each fault patch. In the following excerpt from an input file, all the fault patches use the smoothing parameter $\beta = 0.2$:

```
# no slip   xs      ys    zs length width strike dip   rake
   1 1.34 14.2 -45.43 10.0    5.6  4.94  132.7  91 -114.7
   2 1.89 10.4 -41.31 10.0    5.6  4.94  132.7  91 -151.8
   3 0.46 14.2 -45.41  6.5   3.74  3.53  132.7  91 -150.6
```

but some patches (here, only the second) can be forced to use another value (here, $\beta = 0.5$) as follows:

```
# no slip   xs      ys    zs length width strike dip    rake beta
   1 1.34 14.2 -45.43 10.0    5.6  4.94  132.7  91 -114.7
   2 1.89 10.4 -41.31 10.0    5.6  4.94  132.7  91 -151.8  0.5
   3 0.46 14.2 -45.41  6.5   3.74  3.53  132.7  91 -150.6
```

5.2   Depth-dependent constitutive parameters

The Fourier method used by RELAX to solve the displacement field and the quasi-static velocity field implies homogeneous elastic moduli in the half space. However, all other inelastic or physical parameters, such as viscosity, friction properties and stress, can vary arbitrarily in the domain. RELAX assumes a background depth dependence for these variables. These properties can be modified locally to simulate slabs, ductile zone, or reproduce the gross features of a geological structure.

Let's look at how to define a viscosity profile for a creme brûlée model, with an elastic plate over a viscoelastic half space. First, note that the RELAX input file requires the reference strain rate $\dot{\gamma}_0 = \mu/\eta$, instead of the viscosity η. This is convenient because first, for a purely elastic material, $\dot{\gamma}_0 = 0$, and second, $\dot{\gamma}_0$ is just the reciprocal of the Maxwell relaxation time $t_m = 1/\dot{\gamma}_0$, so one can easily thing in terms of time scales of relaxation, instead of viscosities. The default model is elastic, so it is only necessary to indicate where the lithosphere changes from elastic to viscoelastic

```
# number of linear viscous interfaces (where viscosity changes)
```

```
1
# no depth gammadot0 cohesion
   1  30.0        0.1       0.0
```

Here, we have defined a viscoelastic substrate that extents from $30\,\text{km}$ depth down to the bottom of the computational domain. Assuming that the time units are in year, we have define a uniform viscosity giving rise to a Maxwell time $t_m = 1/0.1 = 10\,\text{yr}$.

Let's look at how to define a viscosity profile for a jelly sandwich model, with a viscoelastic lower crust, a competent, elastic upper mantle, and a viscoelastic asthenosphere. The description of the depth variations of the model is written in a similar way to the PREM model in seismology.

```
# number of linear viscous interfaces for a jelly sandwich strength model
5
# no depth gammadot0 cohesion
   1  15.0        0.1       0.0
   2  30.0        0.1       0.0
   3  30.0        0.0       0.0
   4  70.0        0.0       0.0
   5  70.0        0.2       0.0
```

Here, the lower crust relaxes with a Maxwell time of $t_m = 10\,\text{yr}$, and the asthenosphere with a Maxwell time of $t_m = 5\,\text{yr}$. There is no need to specify the viscosity in the upper $15\,\text{km}$, which is assumed infinite.

6   Examples

6.1   Simple coseismic model

Let's consider first the simplest input model to compute the static deformation due to a left-lateral strike-slip fault. Figure 4 shows the entire input file required to describe the simulation. Note how the code is called, with the command `relax --no-proj-output <<EOF`. In unix, it means that all the text that appears after this line, until the three characters `EOF` are found, is considered as input for the program. In this case, the program is called with the option `--no-proj-output` to indicate that the output does not have to be projected in lat/lon coordinates. It can be useful to call the program with the `--dry-run` option, i.e.,

```
relax --no-proj-output --dry-run <<EOF
# SX1,SX2,SX3 (grid size)
256 256 256
# dx1,dx2,dx3 (km),beta (0-0.5),nq (2)
0.5 0.5 0.5 0.2 2
...
```

to check the geometry of the model. In this case, all the fault patches, the slip distribution and the spatial extent of the grid are exported in the `.vtp` format, which is a standard 3-D geometry format that can be read with such visualization tools as Paraview (`http://www.paraview.org`).

Unless the `--no-vtk-output` option is used, the program exports the displacement field of the entire computational domain in the VTK Legacy binary format for 3-D visualization. For long time-dependent simulation, this output can consume large amount of disk space and it can be useful to discard it with the `--no-vtk-output` option. The stress field is also exported in this format by default. This is cancelled with `--no-stress-output`, but that option cancels out any stress output in GMT format as well.

The standard output of the program is shown in Figure 5. It repeats the details of the input file and adds information such as the recommended maximum sampling size. After the computation, it also outputs one line corresponding to the first time step. It can be useful to save the standard output of the calculation to document what was computed. To do so, one can use the following unix pipeline

```
ODIR=output_directory

relax <<EOF --no-proj-output --no-stress-output | tee $ODIR/in.param
# SX1,SX2,SX3 (grid size)
256 256 256
# dx1,dx2,dx3 (km),beta (0-0.5),nq (2)
0.5 0.5 0.5 0.2 2
# origin position & rotation
0 0 0
# observation depths for displacement and for stress
0 5
# output directory
$ODIR
# lambda (MPa), mu (MPa), gamma (1/km)
...
```

To visualize the coseismic displacement at the surface, it is convenient to use the script `grdmap.sh`. The plotting routine `grdmap.sh` provided with the code and numerous other post-processing scripts can be used to analyze the modeled scenario. The unix script `grdmap.sh`, a wrapper around GMT programs, produces map views of any grid but is optimized to work with the three-dimensional output of RELAX.

```
relax --no-proj-output <<EOF
# SX1,SX2,SX3 (grid size)
256 256 256
# dx1,dx2,dx3 (km),beta (0-0.5),nq (2)
0.5 0.5 0.5 0.2 2
# origin position & rotation
0 0 0
# observation depths for displacement and for stress
0 5
# output directory (all output written here)
output_directory
# lambda (MPa), mu (MPa), gamma (1/km)
3e4 3e4 8.33e-4
# integration time, time step and scaling
0 -1 1
# number of viscous observation slice
0
# number of observation points
0
# number of Coulomb patches
0
# number of prestress interfaces
0
# number of linear viscous interfaces
0
# number of power-law viscous interfaces
0
# number of friction faults
0
# number of interseismic loading strike-slip and opening
0
0
# number of coseismic events (when slip distribution is prescribed)
1
# number of shear dislocations (strike-slip and dip-slip faults)
1
# no slip  xs ys zs length width strike dip rake
   1    1 -10  0  0    10    10       0 90    0
# number of tensile cracks
0
# number of dilatation sources
0
# number of surface traction
0
EOF
```

Figure 4: Input parameters to compute the coseismic deformation due to a left-lateral strike-slip fault with $L = W = 10$ km. The gravity wavelength is defined as $\gamma = (1 - \nu)\rho g/\mu$ where ν is Poisson's ratio, ρ is the density of the crust and g is the acceleration of gravity. The program provides the displacement field and the stress field in multiple formats.

```
--------------------------------------------------------------------------
     nonlinear postseismic relaxation with Fourier-domain Green function
     * Intel MKL implementation of the FFT
     * parallel OpenMP implementation with 016/016 threads
     * export to GRD format
     * export to VTK format
     * export to longitude/latitude text format cancelled (--no-proj-output)
--------------------------------------------------------------------------
grid dimension (sx1,sx2,sx3)
  256  256  256
sampling (dx1,dx2,dx3), smoothing (beta, nyquist)
  5.00E-1  5.00E-1  5.00E-1  2.00E-1  2.00E+0
origin position (x0,y0) and rotation
  0.00E+0  0.00E+0  0.00E+0
observation depth (displacement and stress)
  0.00E+0  5.00E+0
output directory
 output_directory (time report: output_directory/time.txt)
lambda, mu, gamma (gamma = (1 - nu) rho g / mu)
  3.00E+04  3.00E+04  8.33E-04
time interval, (positive time step) or (negative skip, scaling)
  0.00E+0 (output every 001 steps, dt scaled by 1.00E+0)
number of observation planes
    0
...
number of events
    1
number of coseismic strike-slip segments
    1
--------------------------------------------------------------------------
no.    slip      xs       ys       zs  length   width strike   dip   rake
--------------------------------------------------------------------------
001  1.00E+0 -1.00E+1  0.00E+0  0.00E+0 1.00E+1 1.00E+1    0.0  90.0    0.0
--------------------------------------------------------------------------
number of coseismic tensile segments
    0
number of coseismic dilatation point sources
    0
number of surface loads
    0
max sampling size (hor.,vert.): 4.00E+0 4.00E+0
--------------------------------------------------------------------------
coseismic event 001
 I  |   Dt   | tm(ve) | tm(pl) | tm(as) |     t/tmax     | power  | C:E^i |
000* 0.00E+00 0.00E+00 0.00E+00 0.00E+00 0.00E+00/0.00E+0 0.00E+00 3.08E+06
```

Figure 5: Output of the RELAX program for the input parameters shown in Figure 4.

```
grdmap.sh -b -30/30/-30/30 -p -0.05/0.05/0.001 -v 0.5 \
        -u "m" -e erpatch.sh output_directory/000
```

where the $-b$ option defines the boundary of the map in the GMT format W/E/S/N, the $-p$ option defines the range of the color scale for the vertical displacements, the $-v$ option defines the length of the vectors for the horizontal displacement, the "-u" option defines the unit of the color scale, and the "-e" option call the additional script `erpatch.sh` to plot the spatial extent of the fault on the map. The last argument `output_directory/000` refers to the prefix of all GMT binary files associated with the index `000`. Any file prefix followed by `-north.grd`, `-east.grd` and `-up.grd` can be used in this manner. To look at an individual file, for example the stress component σ_{12} at 5 km depth, simply use

```
grdmap.sh -b -30/30/-30/30 -p -500/500/1 \
        -u "kPa" -e erpatch.sh output_directory/000-s12.grd
```

For this command to work, it is assumed that `grdmap.sh` and `erpatch.sh` are both located in a directory listed in the `$PATH` environment variable, such as `/usr/local/bin`.

The coseismic slip distribution of a real earthquake can be a long and detailed description of the source coming from an inversion of geophysical data. To include these models and conform them to the format required by the RELAX program, it is convenient to use other unix tricks, such as `awk`, `wc` and the use of variables, for instance, if the source is described in the file `src.dat`, but the file missing a line counter and the units in meters, one can alter it as follows

```
...
# number of coseismic events
1
# number of shear dislocations
`wc src.dat`
# no slip  xs ys zs length width strike dip rake
`awk '{BEGIN{s=1e3}{print NR,$1/s,$2/s,$3/s,$4/s,$5/s,$6/s,$7,$8,$9}' src.dat`
# number of tensile cracks
0
# number of dilatation sources
0
# number of surface traction
0
EOF
```

The inclusion of unix commands in the input file allows more complex operations, such as filtering out data, shift, rotation and scaling of models, and others. An example complex coseismic slip distribution for the 1992 Mw 7.3 Landers earthquake can be found in the `examples` directory.

6.2 Simple viscoelastic model

Let's extend our simple coseismic model to include a viscoelastic relaxation in a substrate below 30 km. To do so, we need to specify a rheology at depth and indicate how long to simulate the relaxation. RELAX allows two simultaneous viscoelastic relaxation mechanisms, one from a linear rheology

$$\dot{\gamma}^{\text{linear}} = \dot{\gamma}_0 \frac{\tau}{\mu} \tag{17}$$

14

where $\dot{\gamma}^{\text{linear}}$ is the amplitude of the linear viscoelastic strain and $\dot{\gamma}_0$ is a reference strain rate; and another from a power-law rheology

$$\dot{\gamma}^{\text{power-law}} = \dot{\gamma}_0 \left(\frac{\tau}{\mu}\right)^n \tag{18}$$

where n is the power exponent (usually in the range $n = 2 - 5$). In this example, we only use the linear rheology. Choosing a viscosity with a Maxwell time of $t_m = 1/\dot{\gamma}_0 = 1$ yr, we want to compute 20 relaxation times with a time step of $\Delta t = 0.1$ yr. This scenario is specified with the following input lines

```
...
# elastic moduli and gravity parameter
3e4 3e4 8.33e-4
# integration time, time step
20 0.1
# number of observation planes
0
# number of observation points
0
# number of Coulomb patches
0
# number of prestress interfaces
0
# number of linear viscous interfaces
1
# no depth gammadot0 cohesion
   1  30.0       1.0       0.0
# number of linear ductile zones
0
# number of powerlaw viscous interfaces
0
...
```

Note that the time step asked by the program is only the output time step, that is, at what time to output the result. Internally, an optimal time step is always evaluated and the real time step used for the calculation is the smallest of either the internally evaluated value or the time step required to produce an output every multiple of the required time step. The internally evaluated value is always $\Delta t^{\text{internal}} = t_m/10$. Prescribing the output time step can only reduce the computational time step. Note that is a background viscosity has been established, the program requests so called "ductile zones", which are finite volumes where the background viscosity is perturbed. These volumes are described similarly as for a fault, but with an extra "thickness" parameter indicating how the volumes extrudes from the center plane. The standard output of this simulation looks as follows

```
coseismic event 001
 I  |   Dt   | tm(ve) | tm(pl) | tm(as) |     t/tmax     | power  |  C:E^i |
000* 0.00E+00 0.00E+00 0.00E+00 0.00E+00 0.00E+00/2.00E+1 0.00E+00 3.08E+06
001* 1.00E-01 1.00E+00 1.00E+07 1.00E+07 1.00E-01/2.00E+1 4.25E+06 3.50E+06
002* 1.00E-01 1.00E+00 1.00E+07 1.00E+07 2.00E-01/2.00E+1 3.92E+06 3.89E+06
003* 1.00E-01 1.00E+00 1.00E+07 1.00E+07 3.00E-01/2.00E+1 3.63E+06 4.26E+06
004* 1.00E-01 1.00E+00 1.00E+07 1.00E+07 4.00E-01/2.00E+1 3.35E+06 4.59E+06
005* 1.00E-01 1.00E+00 1.00E+07 1.00E+07 5.00E-01/2.00E+1 3.10E+06 4.90E+06
006* 1.00E-01 1.00E+00 1.00E+07 1.00E+07 6.00E-01/2.00E+1 2.88E+06 5.19E+06
007* 1.00E-01 1.00E+00 1.00E+07 1.00E+07 7.00E-01/2.00E+1 2.67E+06 5.45E+06
```

```
008* 1.00E-01 1.00E+00 1.00E+07 1.00E+07 8.00E-01/2.00E+1 2.48E+06 5.70E+06
009* 1.00E-01 1.00E+00 1.00E+07 1.00E+07 9.00E-01/2.00E+1 2.31E+06 5.93E+06
010* 1.00E-01 1.00E+00 1.00E+07 1.00E+07 1.00E+00/2.00E+1 2.15E+06 6.14E+06
011* 1.00E-01 1.00E+00 1.00E+07 1.00E+07 1.10E+00/2.00E+1 2.00E+06 6.34E+06
012* 1.00E-01 1.00E+00 1.00E+07 1.00E+07 1.20E+00/2.00E+1 1.87E+06 6.53E+06
013* 1.00E-01 1.00E+00 1.00E+07 1.00E+07 1.30E+00/2.00E+1 1.74E+06 6.70E+06
014* 1.00E-01 1.00E+00 1.00E+07 1.00E+07 1.40E+00/2.00E+1 1.63E+06 6.86E+06
015* 1.00E-01 1.00E+00 1.00E+07 1.00E+07 1.50E+00/2.00E+1 1.53E+06 7.01E+06
016* 1.00E-01 1.00E+00 1.00E+07 1.00E+07 1.60E+00/2.00E+1 1.43E+06 7.15E+06
017* 1.00E-01 1.00E+00 1.00E+07 1.00E+07 1.70E+00/2.00E+1 1.34E+06 7.28E+06
018* 1.00E-01 1.00E+00 1.00E+07 1.00E+07 1.80E+00/2.00E+1 1.26E+06 7.40E+06
019* 1.00E-01 1.00E+00 1.00E+07 1.00E+07 1.90E+00/2.00E+1 1.18E+06 7.52E+06
020* 1.00E-01 1.00E+00 1.00E+07 1.00E+07 2.00E+00/2.00E+1 1.11E+06 7.63E+06
021* 1.00E-01 1.00E+00 1.00E+07 1.00E+07 2.10E+00/2.00E+1 1.05E+06 7.73E+06
022* 1.00E-01 1.00E+00 1.00E+07 1.00E+07 2.20E+00/2.00E+1 9.88E+05 7.82E+06
023* 1.00E-01 1.00E+00 1.00E+07 1.00E+07 2.30E+00/2.00E+1 9.32E+05 7.91E+06
024* 1.00E-01 1.00E+00 1.00E+07 1.00E+07 2.40E+00/2.00E+1 8.79E+05 7.99E+06
025* 1.00E-01 1.00E+00 1.00E+07 1.00E+07 2.50E+00/2.00E+1 8.31E+05 8.07E+06
026* 1.00E-01 1.00E+00 1.00E+07 1.00E+07 2.60E+00/2.00E+1 7.85E+05 8.15E+06
027* 1.00E-01 1.00E+00 1.00E+07 1.00E+07 2.70E+00/2.00E+1 7.43E+05 8.22E+06
028* 1.00E-01 1.00E+00 1.00E+07 1.00E+07 2.80E+00/2.00E+1 7.03E+05 8.28E+06
029* 1.00E-01 1.00E+00 1.00E+07 1.00E+07 2.90E+00/2.00E+1 6.66E+05 8.35E+06
030* 1.00E-01 1.00E+00 1.00E+07 1.00E+07 3.00E+00/2.00E+1 6.31E+05 8.40E+06
031* 1.00E-01 1.00E+00 1.00E+07 1.00E+07 3.10E+00/2.00E+1 5.98E+05 8.46E+06
032* 1.00E-01 1.00E+00 1.00E+07 1.00E+07 3.20E+00/2.00E+1 5.67E+05 8.51E+06
033* 1.00E-01 1.00E+00 1.00E+07 1.00E+07 3.30E+00/2.00E+1 5.39E+05 8.56E+06
034* 1.00E-01 1.00E+00 1.00E+07 1.00E+07 3.40E+00/2.00E+1 5.11E+05 8.61E+06
035* 1.00E-01 1.00E+00 1.00E+07 1.00E+07 3.50E+00/2.00E+1 4.86E+05 8.65E+06
...
```

The standard output indicates the evaluated Maxwell time (if the viscosity is not uniform, the smallest value of the inferred Maxwell time is used) for the viscoelastic rheology, in the `tm(ve)` column. This value should not evolve throughout the calculation. The time step where output is written to disk are shown with an asterisk, such as `014*`. As the output time step corresponds to the computational time step, the value of the displacement, velocity, stress and other variables are output to disk at every time step. The column `power` is important to check the sanity of the calculation. For a relaxation scenario, the power should reduce at each time step. If not the case, it is symptomatic of a numerical integration error. To correct this, decrease the time steps, or the spatial sampling, or both. The last column is the cumulative moment of inelastic deformation and should always increase.

By default, the deformation is written to disk in map view, for mapping with GMT, or in volume, for 3-D rendering with Paraview, at each step. For time dependent problems, it is convenient for certain points in the domain to save the time series of deformation in a single file. To do so, define "observation points" as follows

```
...
# number of observation planes
0
# number of observation points
3
# no name        x1       x2       x3
 001 GPS1  1.00E+1  0.00E+0  0.00E+0
 002 GPS2  2.00E+1  0.00E+0  0.00E+0
 003 GPS3  3.00E+1  0.00E+0  0.00E+0
```

```
# number of stress observation segments
0
...
```

The observation points are given a four-character name `name` and the time series of displacement and stress is listed in the output file `name.txt`. Using the above example, we obtain

```
> more output_directory/GPS1.txt
#         t           u1        u2        u3        s11         s12         s13
  0.000E+00 -1.736E-05 1.726E-01 -2.343E-08 1.034E-03 -2.199E+03 4.950E-01
  1.000E-01 -1.738E-05 1.726E-01 -2.356E-08 1.035E-03 -2.198E+03 4.950E-01
  2.000E-01 -1.739E-05 1.727E-01 -2.368E-08 1.036E-03 -2.197E+03 4.951E-01
  3.000E-01 -1.741E-05 1.728E-01 -2.376E-08 1.035E-03 -2.197E+03 4.951E-01
...
```

where we have discarded the last three component of the stress tensor in the interest of space. The observation points list the cumulative displacement and stress, including the initial perturbation from an earthquake and the contribution due to the viscoelastic relaxation.

In many cases, the observation points may be the coordinates of GPS stations in a large network or the ground coordinates of the pixels of a synthetic aperture radar interferogram, or some other image of surface deformation. If the location of the surface points are listed in a file `pos.xy`, one can create as many time series with a command such as

```
...
# number of observation points
`wc pos.xy`
# no name         x1        x2        x3
`awk '{printf("%d G%03d %f %f 0\n",NR,NR,$1,$2)}' pos.xy`
# number of stress observation segments
0
...
```

which will create files named `G001.txt`, `G002.txt` and so forth, for each point.

6.3 Simple afterslip model

Let's use RELAX to simulate the deep afterslip that follows a main shock. To do so, we will add a fault below the rupture and assign rate-strengthening properties. We assume that the slip on the fault is governed by a rate-strengthening constitutive law

$$V = 2\,\dot\gamma_0 \, \sinh \frac{\Delta\tau}{(a-b)\sigma} \tag{19}$$

where $\Delta\tau$ is the stress perturbation due to the earthquake, which is slowly relaxed, and $(a-b)\sigma$ and $\dot\gamma_0$ are constitutive parameters. Attention, since $\sinh(x) \sim \exp(x)$ for $x \gg 1$, too small a value for $(a-b)\sigma$ will make the evaluation of the velocity challenging. In this case the execution will stop with an error message indicating a diagnostic value of $\Delta\tau$ and of $(a-b)\sigma$. The time scale of the afterslip scales with

$$t_m^{\text{afterslip}} \propto \frac{L}{2\,\dot s_0} \frac{a\,\sigma}{G} \tag{20}$$

where L is the dimension of the creep area. One can use this scaling relationship to choose the parameters and obtain a reasonable time scale.

An peculiar behavior of this friction law is that the time evolution is non linear, with in some conditions much faster velocities at the early stage of the afterslip transient than at later times. To resolve this numerically, it requires adaptive time steps. To output the simulation at every computational time step, use negative output time steps:

```
...
# integration time, time step and scaling
20 -1 0.5
...
```

In this case, a third argument is needed to modify the internally-evaluated computational time step (here it will be reduced by a half). For example, to output the solution every 10 computational time steps without altering the internal Δt estimate, use

```
...
# integration time, time step and scaling
20 -10 1
...
```

To compute the response of afterslip on a deep extension of the rupture defined in the above examples, use

```
...
# number of nonlinear viscous interfaces
0
# number of fault creep interfaces
1
# no depth   gamma0 (a-b)sig friction cohesion
   1    0      0.3     1e3     0.6        0
# number of afterslip planes
1
# no  x1 x2 x3 length width strike  dip rake
   1 -10  0 11     10    10      0   90   0
# number of inter-seismic strike-slip segments
0
...
```

The standard output reads

```
coseismic event 001
 I  |   Dt   | tm(ve) | tm(pl) | tm(as) |     t/tmax      | power  |  C:Eˆi |
000* 0.00E+00 0.00E+00 0.00E+00 0.00E+00 0.00E+00/2.00E+1 0.00E+00 3.08E+06
001* 1.89E-02 1.00E+07 1.00E+07 3.78E-01 1.89E-02/2.00E+1 1.14E+06 3.10E+06
002* 2.76E-02 1.00E+07 1.00E+07 5.53E-01 4.65E-02/2.00E+1 9.47E+05 3.12E+06
003* 2.97E-02 1.00E+07 1.00E+07 5.94E-01 7.62E-02/2.00E+1 8.06E+05 3.15E+06
004* 2.95E-02 1.00E+07 1.00E+07 5.91E-01 1.06E-01/2.00E+1 7.02E+05 3.17E+06
005* 2.94E-02 1.00E+07 1.00E+07 5.88E-01 1.35E-01/2.00E+1 6.22E+05 3.19E+06
006* 2.93E-02 1.00E+07 1.00E+07 5.86E-01 1.64E-01/2.00E+1 5.57E+05 3.20E+06
007* 2.92E-02 1.00E+07 1.00E+07 5.84E-01 1.94E-01/2.00E+1 5.03E+05 3.22E+06
008* 2.91E-02 1.00E+07 1.00E+07 5.82E-01 2.23E-01/2.00E+1 4.57E+05 3.23E+06
009* 2.90E-02 1.00E+07 1.00E+07 5.80E-01 2.52E-01/2.00E+1 4.17E+05 3.24E+06
010* 2.90E-02 1.00E+07 1.00E+07 5.79E-01 2.81E-01/2.00E+1 3.82E+05 3.25E+06
011* 2.89E-02 1.00E+07 1.00E+07 5.78E-01 3.10E-01/2.00E+1 3.52E+05 3.26E+06
012* 2.88E-02 1.00E+07 1.00E+07 5.77E-01 3.38E-01/2.00E+1 3.25E+05 3.27E+06
013* 2.88E-02 1.00E+07 1.00E+07 5.75E-01 3.67E-01/2.00E+1 3.01E+05 3.28E+06
...
```

and shows a monotonic decrease of the power and a gradual increase of the time steps.

7   Outputs

All GMT output files related to a specific time step are prefixed by the index number, for instance `000-east.grd` is the map view of the east component of deformation for index 0. For each time step, for example index 14, one can find

`014-north.grd`	map view of the north component of cumulative displacement
`014-east.grd`	map view of the east component of cumulative displacement
`014-up.grd`	map view of the vertical component of cumulative displacement
`014-relax-north.grd`	map view of the north component of postseismic displacement
`014-relax-east.grd`	map view of the east component of postseismic displacement
`014-relax-up.grd`	map view of the vertical component of postseismic displacement
`014-s11.grd`	map view of the σ_{11} component of cumulative stress
`014-s12.grd`	map view of the σ_{12} component of cumulative stress
`014-s13.grd`	map view of the σ_{13} component of cumulative stress
`014-s22.grd`	map view of the σ_{22} component of cumulative stress
`014-s23.grd`	map view of the σ_{23} component of cumulative stress
`014-s33.grd`	map view of the σ_{33} component of cumulative stress

The export to files in the GMT binary format `.grd` can be cancelled for the interest of space with the `--no-grd-output` option.

All VTK output files for visualization in Paraview are suffixed with the output index numbers, for example `sigma-0014.vtk`. For each time step, for instance index 14, one can find

`disp-0014.vtk`	subsampled volume of displacement vector
`vel-0014.vtk`	subsampled volume of velocity vector
`sigma-0014.vtk`	subsampled volume of stress tensor
`power-0014.vtk`	subsampled volume of power tensor
`disp-relax-0014.vtk`	subsampled volume of the relaxation part of the displacement vector (no coseismic)

The output `disp-relax-????.vtk` are only available with the `--with-vtk-relax-output` option. The export to files in the VTK binary format `.vtk` can be cancelled for the interest of space with the `--no-vtk-output` option.

Some other files only contain geometrical information, such as geometry of fault patches, grid dimension, position of observation points:

`opts.dat`	list of observation points (coordinates and names)
`rfaults-001.xy`	GMT file containing the slip distribution of event 1
`rfaults-001.vtp`	Paraview file containing the slip distribution of event 1
`rfaults-sigma-0014.vtp`	Paraview file containing the Coulomb stress for time step 14
`aplane-0001.vtp`	Paraview file for the afterslip plane number 1
`linearlayer-001.vtp`	Paraview file for depth of the first linear viscosity change
`cgrid.vtp`	Paraview file for extent of the computational domain
`time.txt`	time associated with time step

The time series of stress and displacement for observation points are in files `NAME.txt`.

8   Benchmarks

The numerical solution produces by RELAX has been compared to many other analytical and numerical solutions. Here, we show two examples for static and time-dependent deformation. In general, it is a good practice to setup simulations using the most resource possible (the largest meshes, the smallest sampling).

8.1   Coseismic deformation

A. Landers surface displacements and numerical error

C. Displacements at 10km depth and numerical error

B. Displacements at 5km depth and numerical error

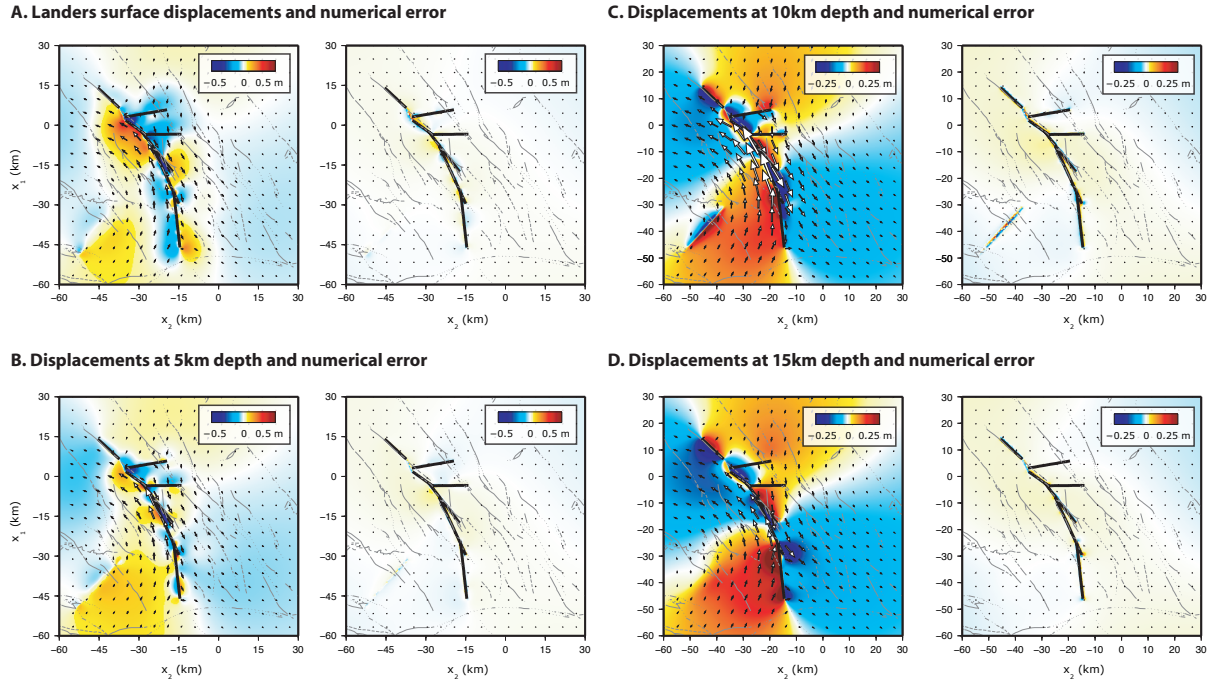**D. Displacements at 15km depth and numerical error**

Figure 6: Simulation of the 1992 Mw 7.3 Landers, CA earthquake. Comparison between the RELAX numerical solution and the solution obtained with the *Okada* [1992] Green's function at the surface (A), and at 5 km (B), 10 km (C) and 15 km depth (D). For each depth the RELAX solution is shown (left) and the residuals with *Okada* [1992]. The arrows indicate horizontal displacement and the color represent vertical displacement (positive up).

Let's consider the coseismic deformation caused by the 1992 Mw 7.3 Landers, CA earthquake. Let's use the slip distribution of [*Fialko*, 2004], which consists in 426 slip patches

```
...
# number of shear dislocations
426
# index slip x1 x2 x3 length width strike dip rake
1 1.3475 14.246 −45.439 10.056 5.6 4.94 132.7 91.0 −114.7
2 1.8921 10.446 −41.319 10.056 5.6 4.94 132.7 91.0 −151.8
3 0.46688 14.201 −45.481 6.5269 3.74 3.53 132.7 91.0 −150.6
4 0.38986 11.668 −42.734 6.5269 3.74 3.53 132.7 91.0 −175.6
5 1.3331 9.1346 −39.987 6.5269 3.74 3.53 132.7 91.0 172.8
...
```

The corresponding input file can be found in the `examples` directory in the file `landers.sh`. Figure 6 shows the comparison between the calculation with RELAX on a 512^3 grid with a sampling of $\Delta x = 0.6$ km and the analytic solution obtained with the *Okada* [1992] Green's function at various depths. The residuals maps reveals some numerical errors in the near field of the rupture caused by the equivalent body-force representation. Some long wavelength error appear at depth (6c,d) caused by the periodicity of the numerical solution due to the Fourier transform method. Overall the residuals are very small, demonstrating the possibility to model accurately geometrically complex earthquake ruptures.

8.2   Non-linear viscoelastic relaxation

Let's look at the postseismic relaxation due to the stress perturbation caused by dip-slip faulting, assuming uniform and isotropic elastic properties for a Poisson's solid (the Lamé parameters are such that $\lambda = G$ and Poisson's ratio is $\nu = 1/4$). The fault slips 1 m uniformly from the surface to a depth of 10 km and is 40 km long. We consider the case of a nonlinear viscoelastic upper mantle governed by the power-law rheology with $n = 2$. We perform the computation with RELAX in a 512^3 grid with a uniform sampling of $\Delta x = 0.8$ km. A snapshot of the surface displacement early in the postseismic transient is shown in Figure 7a. The vertical postseismic displacement has the same polarity as the coseismic displacement. Horizontal postseismic displacements, however, are directed opposite to the coseismic ones. We performed the same simulation using the finite-element software Abaqus and the residuals are shown in the right panel of Figure 7a. The time series of surface postseismic displacements at points numbered from 1 to 8 in the maps are shown in Figure 7b. There is an excellent agreement between the semi-analytic and the finite-element results. The time series are characterized by two striking features. First, initial postseismic velocities are much higher than at later times, as most visible for points 1 and 2. Second, a change in polarity occurs at far-field locations. The change of postseismic displacement orientation is most flagrant for point 6 in the East-West direction. A mild change of polarity can be misleadingly interpreted as a delayed postseismic transient, as for the vertical displacement of point 8, for example.
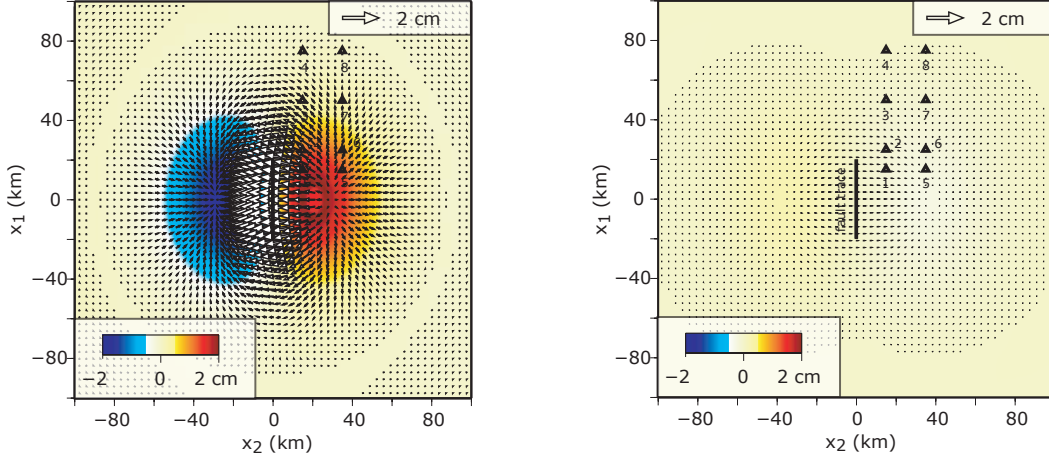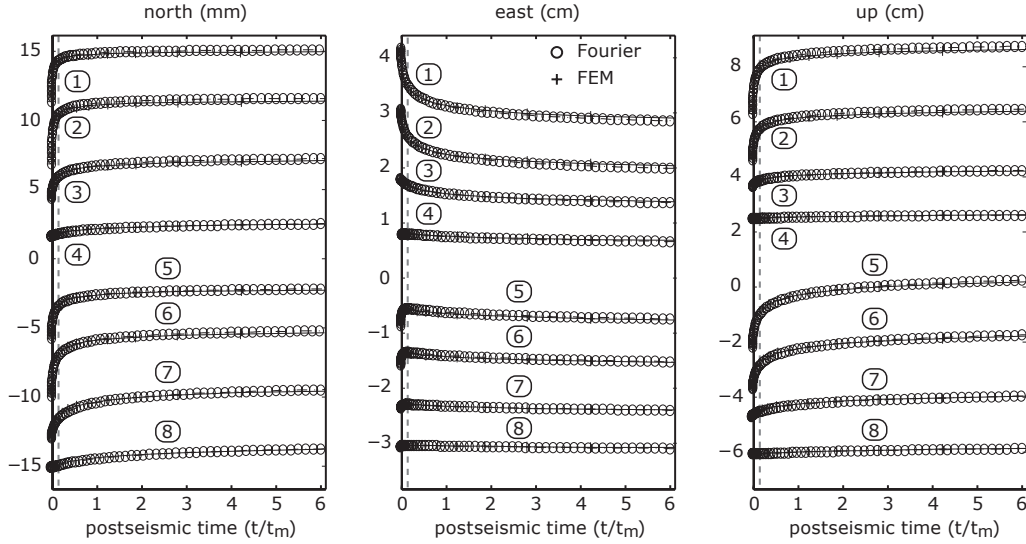
A. Dip-Slip Fault. Powerlaw viscoelasticity (n=2). Displacements and residuals with finite-element calculations

B. Comparison between finite-element and Fourier-domain postseismic time series

Figure 7: Benchmark for time series of surface displacement due to a stress perturbation caused by a dip-slip fault in an elastic plate overriding a nonlinear viscoelastic half space. A vertical dip-slip fault 40 km long extending from the surface to a depth of 10 km slips 1 m. The brittle-ductile transition occurs at a depth of 30 km. The postseismic flow is governed by a power-law rheology with stress exponent $n = 2.0$. Elastic properties are uniform with $\nu = 1/4$. A) A map view of postseismic surface displacements after ten months. A similar computation is performed using finite elements with Abaqus and the residuals are shown in the right panel. B) Time series of surface displacements for the points numbered from 1 to 8 in the corresponding map. The smaller time steps near the onset of the postseismic transient are due to the adaptative time-step procedure. Results from our approach are shown every 5 computation steps for clarity. The residuals between results from our numerical approach and the finite element calculation are less than 5% and show reasonable agreement both in map view and in time.

References

Aki, K., and P. G. Richards, *Quantitative Seismology*, vol. I, W. H. Freeman and company, New York, 1980.

Barbot, S., and Y. Fialko, Fourier-domain Green function for an elastic semi-infinite solid under gravity, with applications to earthquake and volcano deformation, *Geophys. J. Int.*, doi:10.1111/j.1365-246X.2010.04655.x, 2010a.

Barbot, S., and Y. Fialko, A unified continuum representation of postseismic relaxation mechanisms: semi-analytic models of afterslip, poroelastic rebound and viscoelastic flow, *Geophys. J. Int.*, doi:10.1111/j.1365-246X.2010.04678.x, 2010b.

Barbot, S., Y. Fialko, and Y. Bock, Postseismic deformation due to the Mw 6.0 2004 Parkfield earthquake: Stress-driven creep on a fault with spatially variable rate-and-state friction parameters, *J. Geophys. Res.*, *114*(B07405), doi:10.1029/2008JB005748, 2009a.

Barbot, S., Y. Fialko, and D. Sandwell, Three-dimensional models of elasto-static deformation in heterogeneous media, with applications to the Eastern California Shear Zone, *Geophys. J. Int.*, *179*(1), 500–520, 2009b.

Bruhat, L., S. Barbot, and J. P. Avouac, Evidence for postseismic deformation of the lower crust following the 2004 Mw6.0 Parkfield earthquake, *J. Geophys. Res.*, *116*, 10, 2011.

Fialko, Y., Evidence of fluid-filled upper crust from observations of post-seismic deformation due to the 1992 M_w7.3 Landers earthquake, *J. Geophys. Res.*, *109*, B08,401, 10.1029/2004JB002,985, 2004.

Mogi, K., Relations between the eruptions of various volcanoes and the deformations of the ground surfaces around them, *Bull. Earthquake Res. Inst. Univ. Tokyo*, *36*, 99–134, 1958.

Okada, Y., Internal deformation due to shear and tensile faults in a half-space, *Bull. Seism. Soc. Am.*, *82*, 1018–1040, 1992.

Wang, R., F. Martin, and F. Roth, Computation of deformation induced by earthquakes in a multi-layered elastic crust - FORTRAN programs EDGRN/EDCMP, *Comp. Geosci.*, *29*, 195–207, 2003.

Wang, R., F. Lorenzo-Martin, and F. Roth, PSGRN/PSCMP-a new code for calculating co- and post-seismic deformation, geoid and gravity changes based on the viscoelastic-gravitational dislocation theory, *Computers and Geosciences*, *32*, 527–541, 2006.